Ceramics-Silikáty 64 (4), 407-417 (2020)
www.ceramics-silikaty.cz doi: 10.13168/cs.2020.0028

# EMPIRICAL MODELLING OF THE COMPRESSIVE STRENGTH OF AN ALKALINE ACTIVATED NATURAL POZZOLAN AND LIMESTONE POWDER MORTAR

ADESHINA ADEWALE ADEWUMI*, MOHAMMAD ISMAIL*, MOHD AZREEN MOHD ARIFFIN**,
#MORUF OLALEKAN YUSUF***, HAMZA ONORUOIZA SALAMI****,
TAOREED O. OWOLABI*****, MOHAMMED MASLEHUDDIN******

*School of Civil Engineering, Faculty of Engineering, Universiti Teknologi Malaysia, 81310 UTM Johor Bahru, Johor, Malaysia
**School of Civil Engineering, Forensic Engineering Centre, Faculty of Engineering, Universiti Teknologi Malaysia, 81310 UTM Johor Bahru, Johor, Malaysia
***Department of Civil Engineering, University of Hafr Al Batin, 31991 Hafr Al-Batin, Saudi Arabia
****College of Computer Science and Engineering, University of Hafr Al-Batin, Hafar Al-Batin 31991, Saudi Arabia
*****Physics and Electronics Department, Adekunle Ajasin University, Akungba Akoko, Ondo State, Nigeria
******Center for Engineering Research, Research Institute, King Fahd University of Petroleum and Minerals, 31261 Dhahran, Saudi Arabia

#E-mail: moruf@uhb.edu.sa

Submitted April 17, 2020; accepted June 8, 2020

**Keywords:** Alkaline-activated, Compressive strength, Stepwise-regression, Genetic algorithm, Natural-pozzolan and limestone powder

*An experimental investigation was conducted to synthesise an alkali-activated binder using natural pozzolan and limestone powder. The effect of the mix parameters such as the binder ratio, NaOH molarity (4 - 14 M), curing temperature (25 - 90 °C), sodium silicate to sodium hydroxide ratio (0.5 - 1.5), fine aggregate to binder ratio (1.4 - 2.2), alkaline activator to binder ratio (0.45 - 0.55) and curing days (1, 3, 7, 14, 28) were determined on the compressive strength of the mortar. A stepwise regression algorithm was developed to estimate the compressive strength of the mortar. Five different models (I-V) were developed using 130 experimental data sets with seven descriptors. Bayesian information criterion (BIC), Akaike's information criterion (AIC) and the sum of square error (SSE) criteria were used to fit the developed model in order to select the best model. The cubic with interactions model (V) is characterised with a high correlation coefficient (97.2 %), the lowest root means square error (1.672), and the lowest mean absolute error (1.313) in comparison with the other four models (I-IV). The outcomes of this work could provide an effective and efficient way of modelling the compressive strength of environmentally friendly binders with minimal experimental stress, limit the uncertainties and errors inherent in a laboratory.*

## INTRODUCTION

The ordinary Portland cement (OPC) manufacturing process is energy-intensive [1]. The calcination of calcium carbonate during the OPC production significantly leads to 5 - 8 % of the global $CO_2$ emissions into the atmosphere, which poses a serious danger to the world ecological systems [2,3]. A high demand for cement from emerging countries, especially China and the developing nations have helped to mount pressure on the cement industries to improve the cement production energy efficiency and also to find alternative raw materials for the manufacturing of the cement [1,4]. Despite the inevitability of using concrete in construction industries, the environmental danger of conventional ordinary Portland cement is of a serious concern, which necessitates urgent attention to search for alternative binders. Alkali-activated materials have been identified as a potential alternative to ordinary Portland cement due to their environmental friendliness, excellent compressive strength and low permeability.

Alkali-activated materials (AAM) are materials containing significant amounts of alumina and silica. AAM is activated using alkaline solutions, the alkali activation process involves three main stages; the first stage is the dissolution of the solid aluminosilicate precursor, followed by the polymerisation of monomers and oligomers, and finally the polycondensation and stabilisation of the cross-linked networks of monomers and oligomers reorganisation [5]. AAM has emerged as a new alternative binder to OPC due to its lower environmental impact, excellent strength development, good thermal resistance, innocuity to alkaline-aggregate reactions and low permeability [6–8]. The synthesis of alkali-activated binders using the world's vast deposit of natural

pozzolan (NP) [9–11], rice husk ash [12], palm oil fuel ash (POFA) [12–16], silico-manganese slag [17], ground granulated blast furnace slag [17–19], fly ash [20], and silica fume [20,21] will contribute to waste valorisation, dumpsite land reclamation, and a reduction in the environmental hazards. AAM is gaining a wide range of applications in precast concrete and for in-situ construction. About 40 000 $m^3$ of geopolymer concrete was used for the construction of the heavy-duty pavement at the Brisbane West Well camp Airport in Australia [22]. In addition, several road infrastructure projects were constructed using a geopolymer by VicRoads State Agency in Australia [23]. Furthermore, several applications and the standardisation of AAM are still in progress in Russia, the Ukraine, South Africa, the Netherlands, the UK and the USA [24–26].

The compressive strength (CS) of AAM is of great significance to design engineers because it is one of the key mechanical properties that determine its suitability for structural purposes. The CS of an alkali-activated mortar (AAMT) is a function of many parameters, such as the oxide compositions of the primary based materials (precursor), sodium hydroxide molarity (NH), the curing temperature, sodium silicate to sodium hydroxide ratio (NS/NH) or the silica modulus, the alkaline to binder ratio [NS + NH)/BD], the fine aggregate to binder ratio (FA/BD), the water to binder ratio (W/BD) and the curing duration [9, 14, 27]. The synthesis of an alkali-activated mortar by using traditional laboratory procedures for the acquisition of its mechanical properties is labourious, expensive and time-consuming. This is because, the processes involve the preparation, curing and testing of several samples [28]. Quite a lot of work on the synthesis of AAMT has focused on the experimental aspect more in order to understand the roles played by the previously mentioned parameters on the compressive strength of the paste, mortar and concrete. Many researchers have experimentally synthesised alkali-activated mortars and concrete from natural pozzolan (NP) [9,10,29–31], rice husk ash [12], palm oil fuel ash (POFA) [12–16], silico-manganese slag (SiMn) [17], ground granulated blast furnace slag (GGBFS) [17–19,32,33], fly ash (FA) [20], and silica fume (SF) [20,21].

In the previous studies, artificial neural networks (ANN) and regression analysis (RA) have been used to predict the AAM compressive strength of blast furnace slag and fly ash concrete [34]. RA has been used for correlating the steel-concrete bond strength to the mean compressive strength of OPC and geopolymer concretes [35]. The compressive strength of the concrete has also been estimated using ANN [36]. Furthermore, the compressive strength of structural lightweight concrete was predicted using ANN [37], as well as the rheology of self-compacting concrete [38]. However, ANN is associated with some draw-backs such as a slow learning rate, a complex design, random initialisation, non-convergence to a local minimal, it also requires a large dataset for a better generalisation apart from its hidden predictive equations – a similitude of an airplane black box [39].

Stepwise-regression analysis is used in expressing the correlation between the independent variables or input (predictors) and the dependent variables or outputs (response). It can either be linear or nonlinear regression. Linear regression is very simple, but characterises with low prediction accuracy and this is in antithesis to the nonlinear regression. Examples of nonlinear functions include exponential functions, trigonometric functions, logarithm and power functions. Thomas and Peethamparan developed a step-wise regression model for predicting the compressive strength of alkaline activated fly-ash and slag using four descriptors [40]. However, the developed model failed to consider the effect of the molarity, the wide range of curing temperatures and the curing duration. Generally, regression methods give explicit equations that can be utilised by structural engineers to design the models. RAs are computationally efficient when the predictors are small in number. However, when the input parameters are large with complex variable interdependency, the accuracy of the model could be very low due to the over-fitting. Over-fitting is a problem that occurs when the training model has a very small training error, but has a large validation error.

It is an obvious fact that the research in AAM mix design is a labourious exercise, time-consuming and leads to a waste of scarce resources. In view of this, it is extremely important to develop a theoretical estimation model for the compressive strength of AAMT, this will go a long way in reducing the time, energy and cost for the preparation and testing of the samples. In this present work, natural pozzolan (NP) and limestone waste powder (LSPW) solid wastes are used to synthesise the alkaline-activated mortar. NP is a by-product from volcanic eruptions, while limestone powder is a waste from tile manufacturing industries. Alkali-activated binder synthesised between silica containing compounds, such metakaolin and natural pozzolan, with a calcium compound, such as limestone powder, will lead to the formation of an aluminosilicate framework in which the LSP ($Ca^{2+}$) acts as a charge balance in the formed skeletal framework leading to formation of C–A–S–H or N–A–SH [5,31]. This work develops a stepwise-regression model for the estimation of the compressive strengths of alkali-activated natural pozzolan/limestone powder mortar (AANLM). The descriptive input parameters include: the binary binder variation ($x$), sodium hydroxide molarity (NH), curing temperature, sodium silicate to sodium hydroxide ratio (NS/NH), alkaline to binder ratio [(NS + NH)/BD], fine aggregate to binder ratio (FA/BD), water to binder ratio (W/BD) and the curing duration on the compressive strength of AANLM. The developed models using BIC and SSE show excellent results with a high coefficient of correlation, low root means square error and low mean absolute error.

## EXPERIMENTAL

### Description of the raw binder materials

The natural pozzolan (NP) used for this research was provided by Imerys Minerals Arabia, the Kingdom of Saudi Arabia (KSA) and the limestone powder waste (LSPW) was obtained as a powder formed from the tile industry. The physical and the chemical compositions of the precursor are presented in Table 1 and Table 2. The particle size distributions (PSDs) of the precursor is shown in Figure 1. The mineralogical composition and amorphous or crystalline nature of the raw materials were explored using X-ray diffraction (XRD) analysis and the result is shown in Figure 2. The NP mainly contains quartz, $SiO_3$, plagioclase ($(Ca, Na)Al_2Si_2O_8$) and microcline ($KAl_2Si_2O_8$), it also revealed that the NP is amorphous in nature with very low crystallinity. The LSPW mainly comprises calcite ($CaCO_3$) and quartz ($(SiO_2$) with a high level of crystallinity.

### Synthesis of alkaline activator

The alkaline activators used in this study are a combination of a commercially available aqueous sodium silicate (NS) and $NaOH_{(aq)}$ (NH) of different molarities (4M, 6M, 8M, 10M, 12M and 14M). The initial silica modulus (Ms = $SiO_2/Na_2O$) of the SS is 3.3 and its percentage composition of the $Na_2SiO_{3(aq)}$ are as follows: $H_2O$: 62.11 %, $SiO_2$: 29.13 % and $Na_2O$: 8.76 %.

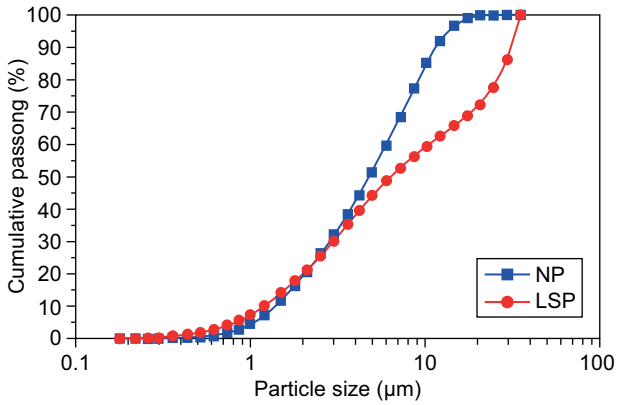


Figure 1. The particle size distribution of the based materials.

Table 1. The physical properties of the NP and LSPW.

| Materials | Specific gravity | Average particle size, $d_{50}$ (μm) | Specific surface area ($cm^2 \cdot g^{-1}$) |
|---|---|---|---|
| NP | 2.3 | 4.84 | 3.1 |
| LSWP | 2.7 | 6.43 | 0.6 |

### Aggregates

Dune desert sand passing the gradation size requirement of ASTM C33 [41] was used as the fine aggregate (FA). The fineness modulus of the FA was 1.82 while the specific gravity in saturated surface dry (SSD) condition was 2.63.

### Mix design, sample preparation and testing

The mixture proportions of the alkali-activated mortar were designed with an LSPW content of 0 %, 20 %, 40 %, 60 % 80 % and 100 % (natural pozzolan contents of 100 %, 80 %, 60 %, 40 %, 20 % and 0 %, respectively). The samples were designated as alkali-activated NP/LSPW mortar ($AANL_x$), where $x$ is the L/(L+N) ratio, while $x$ varied as 0, 0.2, 0.4, 0.6. 0.8 and 1. The fine aggregate-to-the binder (FA/B) ratio ranges from 1.4 to 2.2 at an interval of 0.2. The alkaline activator (NS/NH) ratio ranges from 0 to 1.25 while the alkaline activator to binder ratio (NS+NH)/(L+N) varied at 0.45, 0.5 and 0.55. The free water to the precursor (pozzolanic material) ratio was kept as 10 % of the total base materials (L+N) in all the mixtures. The curing temperatures were 25, 45, 60, 75, and 90 °C at constant duration of 24 hrs before being placed under laboratory exposure condition at 20 ± 5 °C until the age of testing

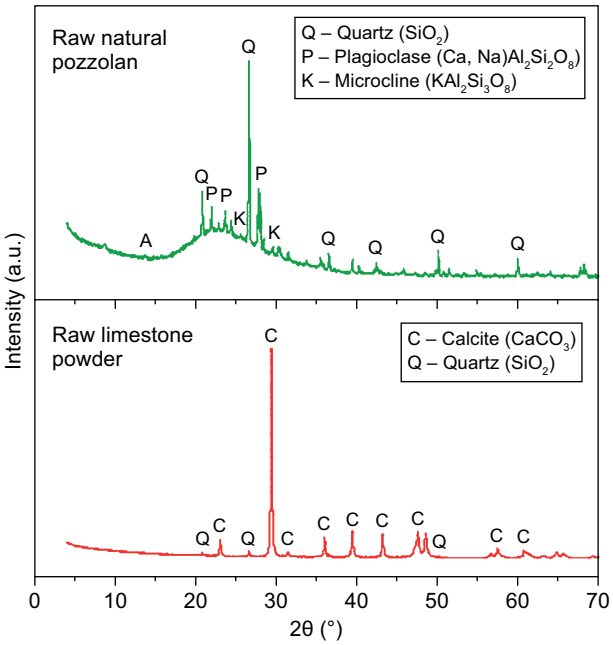


Figure 2. The X-ray diffractograms: a) raw natural pozzolan and b) raw limestone powder.

Table 2. The chemical compositions of the NP and LSPW obtained from XRF.

| Oxides | $SiO_2$ | CaO | $Al_2O_3$ | $Fe_2O_3$ | MgO | $Na_2O$ | $K_2O$ | $SO_3$ | L.O.I |
|---|---|---|---|---|---|---|---|---|---|
| LSPW (%) | 2.5 | 94.1 | 0.8 | 1.2 | 0.6 | – | 0.3 | 0.5 | 44 |
| NP (%) | 74 | 2 | 13 | 1.5 | 0.5 | 4 | 5 | – | 5 |

(1, 3, 7, 14 and 28 days). The compressive strengths of the AANL mortar was determined in accordance with ASTM C 150 [42] on 50 × 50 × 50 $mm^3$ cube specimens using a digital compression testing machine. The mixture proportions and the range of the input parameters are summarised in Table 3. The average of the triplicate specimens was recorded as the compressive strength. Table 4 summarises the proportion of the mix design and the compressive strengths of the 25 mixtures generating a total of 130 data sets for the different ages (1, 3, 7, 14 and 28 days).

## THEORETICAL

### Descriptions of the proposed model

#### *Stepwise regression algorithm*

Stepwise regression is an automatic way of building predictive regression models in which the appropriate subset of variables to be used for the prediction are systematically determined based on some specified criterion. There are two common approaches for carrying out stepwise regression: forward selection and backward elimination [40]. On one hand, models are built during

Table 3. The mixture proportion variables and ranges.

| SN | Input parameter | Notation | Ranges |
|---|---|---|---|
| 1 | Binder ratio (*x*) | X | 0, 0.2, 0.4, 0.6, 0.8 ,1 |
| 2 | NaOH molarity (mol $dm^{-3}$) | M | 4, 6, 8, 10, 12, 14 |
| 3 | Moist and heat curing temperature (°C) | T | 25, 45, 60, 75, 90 |
| 4 | Sodium silica to sodium hydroxide ratio | NS/NH | 0.5, 0.75, 1, 1.25, 1.5 |
| 5 | Fine aggregate to binder ratio | FA/B | 1.4, 1.6, 1.8, 2.0, 2.2 |
| 6 | alkaline activator to binder ratio | AK/B | 0.45, 0.5, 0.55 |
| 7 | Curing age (days) | D | 1, 3, 7, 14, 28 |

Table 4. The mixture proportions of the alkali-activated natural pozzolan/limestone powder waste mortar.

| Mix | X* | M (mol·$dm^{-3}$) | T (°C) | NS/NH | FA/B | AK/B | CS-1 (MPa) | CS-3 (MPa) | CS-7 (MPa) | CS-14 (MPa) | CS-28 (MPa) |
|---|---|---|---|---|---|---|---|---|---|---|---|
| M1 | 0 | 10 | 75 | 1 | 2 | 0.5 | 4.4 | 4.9 | 5.2 | 7.4 | 8.9 |
| M2 | 0.2 | 10 | 75 | 1 | 2 | 0.5 | 18.6 | 18.7 | 21.9 | 22.4 | 22.6 |
| M3 | 0.4 | 10 | 75 | 1 | 2 | 0.5 | 20.7 | 23.9 | 24.3 | 24.5 | 25.0 |
| M4 | 0.6 | 10 | 75 | 1 | 2 | 0.5 | 20.9 | 24.0 | 25.2 | 25.3 | 27.0 |
| M5 | 0.8 | 10 | 75 | 1 | 2 | 0.5 | 12.9 | 14.0 | 14.5 | 15.3 | 15.7 |
| M6 | 1 | 10 | 75 | 1 | 2 | 0.5 | 5.3 | 5.6 | 5.8 | 6.0 | 6.3 |
| M7 | 0.6 | 4 | 75 | 1 | 2 | 0.5 | 4.3 | 4.4 | 4.8 | 5.3 | 6.0 |
| M8 | 0.6 | 6 | 75 | 1 | 2 | 0.5 | 4.7 | 4.9 | 5.0 | 5.6 | 7.6 |
| M9 | 0.6 | 8 | 75 | 1 | 2 | 0.5 | 7.9 | 8.4 | 9.0 | 9.8 | 11.6 |
| M10 | 0.6 | 12 | 75 | 1 | 2 | 0.5 | 20.2 | 24.3 | 24.7 | 24.7 | 22.8 |
| M11 | 0.6 | 14 | 75 | 1 | 2 | 0.5 | 21.6 | 23.6 | 24.7 | 24.0 | 22.7 |
| M12 | 0.6 | 10 | 25 | 1 | 2 | 0.5 | 6.85 | 7.73 | 10.55 | 11.68 | 13.00 |
| M13 | 0.6 | 10 | 45 | 1 | 2 | 0.5 | 10.68 | 12.47 | 12.76 | 13.25 | 14.13 |
| M14 | 0.6 | 10 | 60 | 1 | 2 | 0.5 | 17.06 | 19.34 | 20.36 | 20.86 | 22.00 |
| M15 | 0.6 | 10 | 90 | 1 | 2 | 0.5 | 23.35 | 24.13 | 24.37 | 24.84 | 25.92 |
| M16 | 0.6 | 10 | 75 | 0 | 2 | 0.5 | 9.6 | 14.4 | 13.2 | 14.3 | 15.6 |
| M17 | 0.6 | 10 | 75 | 0.5 | 2 | 0.5 | 15.4 | 18.3 | 18.9 | 19.1 | 18.9 |
| M18 | 0.6 | 10 | 75 | 0.75 | 2 | 0.5 | 17.1 | 19.1 | 19.0 | 19.5 | 20.4 |
| M19 | 0.6 | 10 | 75 | 1.25 | 2 | 0.5 | 18.3 | 18.9 | 18.8 | 15.3 | 16.2 |
| M20 | 0.6 | 10 | 75 | 1.5 | 2 | 0.5 | 10.9 | 12.3 | 13.4 | 10.5 | 10.9 |
| M21 | 0.6 | 10 | 75 | 1 | 1.4 | 0.5 | 15.4 | 18.3 | 20.1 | 22 | 23.5 |
| M22 | 0.6 | 10 | 75 | 1 | 1.6 | 0.5 | 17.6 | 20.6 | 22.4 | 23.3 | 24.3 |
| M23 | 0.6 | 10 | 75 | 1 | 1.8 | 0.5 | 18.2 | 21.2 | 23.6 | 24.2 | 25 |
| M24 | 0.6 | 10 | 75 | 1 | 2.2 | 0.5 | 19.5 | 21.3 | 22.8 | 23.4 | 24.4 |
| M25 | 0.6 | 10 | 75 | 1 | 2 | 0.45 | 20.3 | 22.2 | 23.7 | 25.0 | 23.7 |
| M26 | 0.6 | 10 | 75 | 1 | 2 | 0.55 | 21.5 | 23.6 | 22.8 | 23.1 | 22.5 |

** The ratio of the limestone powder to the total base materials*

forward selection by beginning with a constant and continuously including the other parameters with a view to gaining a better fit. On the other hand, backward elimination commences with all the parameters and then continuously removes those of insignificant contribution to the fit. Three criteria were used to measure the accuracy of the developed models which include: the sum of the squared error, Bayesian Information Criteria and Akaike Information Criteria.

*Sum of Squared Error (SSE)*

The sum of squared error (SSE) is a commonly used measure for estimating the predictive performance of a model. As shown in Equation 1, it is the sum of the square of the difference between the model output ($Y_{est}$) and the actual experimental values ($Y_{exp}$).

$$SSE = \frac{1}{n}\sum_{i=i}^{n}[Y_{(est)}(i) - Y_{(exp)}(i)]^2 \quad (1)$$

*Bayesian Information Criteria (BIC)*

The Bayesian Information Criteria (BIC) is another popular yardstick for determining the model fit. It is based on the likelihood function $L$, which measures the probability that the data comes from a particular population, given a certain model. BIC tackles the problem of model over-fitting [40] by immensely penalising for the number of terms in the model. Over-fitting is the ability of a model to fit exactly or very closely to a given set of data, yet the model performs poorly on the other sets of data. BIC can be computed using Equation 2, where $k$ is the number of model terms and $n$ is the sample size. The desired model is the one which minimises the BIC.

$$\mathrm{BIC} = k \ln(n) - 2\ln(L) \quad (2)$$

*Akaike Information Criteria (AIC)*

The Akaike Information Criteria **(**AIC) is closely related to the BIC. Both AIC and BIC balance between the goodness of the fit (likelihood function) and the over-fitting (mainly estimated from the number of model terms $k$). However, as can be seen from the first terms on the right-hand side of Equations 2 and 3, AIC has a smaller penalty for over-fitting, when compared to BIC.

$$\mathrm{AIC} = 2k - 2\ln(L) \quad (3)$$

Criteria for generalising the performance of the developed models

For the assessment of the accuracy of the developed stepwise-regression models, the root mean square error (RMSE), mean absolute error (MAE) and the coefficient of correlation (CC) were used as shown in Equations 4-6, respectively.

$$RMSE = \sqrt{\frac{1}{m}\sum_{j=1}^{m} Er_i^2} \quad (4)$$

$$MAE = \frac{1}{m}\sum_{j=1}^{m}\left|Er_j\right| \quad (5)$$

$$CC = \frac{\sum_{j=1}^{m}\left(V_{j\,(\exp)} - V'_{(\exp)}\right)\left(V_{j\,(\mathrm{est})} - V'_{(\mathrm{est})}\right)}{\sqrt{\sum_{j=1}^{m}\left(V_{j\,(\exp)} - V'_{(\exp)}\right)^2 \sum_{j=1}^{m}\left(V_{j\,(\mathrm{est})} - V'_{(\mathrm{est})}\right)^2}} \quad (6)$$

where $Er_j$ represents the difference between the experimental and estimated compressive strength value and $m$ stands for the total number of data points. $V_{j(\exp)}$ and $V_{j(\mathrm{est})}$ respectively represent the experimental and the estimated compressive strength while $V'_{(\exp)}$ and $V'_{(\mathrm{est})}$ stand for their mean values, respectively.

Description of the dataset

The training, validation and testing stages of the developed predictive models (model I, model II, model III, model IV and model V) were performed using the dataset contained in Appendix 1. The stepwise-regression training, validation and testing models were developed using 130 data-points with seven inputs parameters or descriptors for the prediction of the compressive strength. These include the binary binder variation (percentage combination of the NP and LSPW), sodium hydroxide molarity (M), curing temperature (T), sodium silicate to sodium hydroxide ratio (NS/NH), alkaline to binder ratio [NS + NH)/BD], fine aggregate to binder ratio (FA/BD), water to binder ratio (W/BD) and the curing duration (D).

The descriptors used for the developed model are important parameters that influence the compressive strength performance of alkaline-activated binders. The proposed model incorporates several factors which are yet to be reported in the literature. This makes the developed model in this study more robust.

Computational methodology for model training, validation and testing

The normalisation of the dataset was undertaken in order to improve the prediction capacity and the efficiency of the developed model, which was carried out using stepwiselm in MATLAB. The randomisation of the dataset was undertaken by dividing the data into 70 % of the training set, 15 % of the validation set and 15 % of the testing set. The training data set was used to build five classes of the predictive model as shown below:

I. *Linear without interactions:* The model can have an intercept, as well as a linear term for each input parameter.
II. *Linear with interactions:* The model may contain an intercept, as well as a linear term for each input parameter, and all the products of pairs of distinct input parameters (no squared terms).

III. *Pure Quadratic:* The model can contain an intercept term, as well as linear and squared terms for each input parameter.

IV. *Quadratic with interaction:* The model may have an intercept term, as well as linear and squared terms for each predictor, and all the products of the pairs of distinct predictors.

V. *Cubic with interactions:* The model may have an intercept term, as well as linear, squared and cubed terms for each input parameter, and all the products of the pairs of distinct input parameters.

The Bayesian information criterion (BIC), Akaike's information criterion (AIC) and sum of the square error (SSE) criteria were used to fit the developed model from which the best choice is selected using CC, RMSE and MAE. Figure 3 shows the step by step procedures used in developing each of the models:

1. Start
2. Split dataset into training, validation and test datasets
3. **for each** criterion *cr* in {***SSE***, ***AIC***, ***BIC***} **do**
4. **for each** model *mdl* in {linear – interactions, linear + interactions, pure
5. quadratic, quadratic + interactions, cubic + interaction} **do**
6. Build forward selection stepwise regression model from training set using *cr* and *mdl*
7. Record performance of stepwise model on training, validation and test sets
8. *bestModelEquation* ← model with best performance on validation set so far
9. **end for**
10. **end for**
11. Output *bestModelEquation*

Figure 3. The computational methodology of the developed models.

## RESULTS AND DISCUSSION

### Evaluation of the generalisation and predictive capacity of the developed models

The correlation coefficient (CC), root means square error (RMSE) and mean absolute error (MAE) were used to evaluate the predictive capacity of all the developed models under the influence of a fitting criteria (BIC, AIC, and SSE). Generally, the accuracy of all the models increases as the order of the equation increases using the three fitting criteria. Considering the CC values of the BIC models, an accuracy of 61.4 %, 80.1 % and 53.6 % were obtained during the training, validation and testing, respectively, for the linear without interactions model (model I) as shown in Table 5. Similar values were obtained for the linear with interactions model (model II). However, when the order of the model changed to second-order (model III and IV), the accuracy of the model improved by 48.86 %, 15.73 %, and 72.39 % for the training, validation and testing, respectively (Tab. 5). The cubic with interactions model (model V) gave the best predictive model with an accuracy of 96.6 %, 97.8 % and 97.2 % during the training, validation and testing of the developed model. Similar trends were observed using the RMSE and the MAE as shown in Table 5. Furthermore, using the SSE and AIC as fitting criteria, the accuracy of all the models increases as the order of the equation increases (Tables 6 and 7). Model V showed excellent performance with high values of CC and low values of RMSE and MAE when compared with the models (I-IV) (Tables 6 and 7).

The best testing model (model V) was used to compare the predictive strength of the developed model.

Table 5. The model performance during the training, validating and testing phases of the stepwise regression model using the Bayesian information criterion (BIC).

| Model | Training CC | Validation CC | Testing CC | Training RMSE (MPa) | Validation RMSE (MPa) | Testing RMSE (MPa) | Training MAE (MPa) | Validation MAE (MPa) | Testing MAE (MPa) |
|---|---|---|---|---|---|---|---|---|---|
| Linear – interactions | 0.614 | 0.801 | 0.536 | 5.117 | 5.386 | 5.263 | 4.123 | 4.597 | 4.060 |
| Linear + interactions | 0.614 | 0.801 | 0.536 | 5.117 | 5.386 | 5.263 | 4.123 | 4.597 | 4.060 |
| Pure quadratic | 0.914 | 0.927 | 0.924 | 2.623 | 3.386 | 2.411 | 2.148 | 2.894 | 2.083 |
| Quadratic + interactions | 0.914 | 0.927 | 0.924 | 2.623 | 3.386 | 2.411 | 2.148 | 2.894 | 2.083 |
| Cubic + interactions | 0.966 | 0.978 | 0.972 | 1.682 | 1.741 | 1.672 | 1.309 | 1.368 | 1.313 |

Table 6. The model performance during the training, validating and testing phases of the stepwise regression model using the Sum of the square error (SSE).

| Model | Training CC | Validation CC | Testing CC | Training RMSE (MPa) | Validation RMSE (MPa) | Testing RMSE (MPa) | Training MAE (MPa) | Validation MAE (MPa) | Testing MAE (MPa) |
|---|---|---|---|---|---|---|---|---|---|
| Linear – interactions | 0.632 | 0.827 | 0.549 | 5.025 | 5.205 | 5.210 | 4.076 | 4.512 | 4.131 |
| Linear + interactions | 0.632 | 0.827 | 0.549 | 5.025 | 5.205 | 5.210 | 4.076 | 4.512 | 4.131 |
| Pure quadratic | 0.914 | 0.927 | 0.924 | 2.623 | 3.386 | 2.411 | 2.148 | 2.894 | 2.083 |
| Quadratic + interactions | 0.914 | 0.927 | 0.924 | 2.623 | 3.386 | 2.411 | 2.148 | 2.894 | 2.083 |
| Cubic + interactions | 0.966 | 0.978 | 0.972 | 1.682 | 1.741 | 1.672 | 1.309 | 1.368 | 1.313 |

Table 7. The model performance during the training, validating and testing phases of the stepwise regression model using the Akaike's information criterion (AIC).

| Model | Training CC | Validation CC | Testing CC | Training RMSE (MPa) | Validation RMSE (MPa) | Testing RMSE (MPa) | Training MAE (MPa) | Validation MAE (MPa) | Testing MAE (MPa) |
|---|---|---|---|---|---|---|---|---|---|
| Linear - interactions | 0.632 | 0.827 | 0.549 | 5.025 | 5.205 | 5.210 | 4.076 | 4.512 | 4.131 |
| Linear + interactions | 0.651 | 0.759 | 0.435 | 4.920 | 5.483 | 6.661 | 3.910 | 4.739 | 5.083 |
| Pure quadratic | 0.918 | 0.939 | 0.910 | 2.566 | 3.073 | 2.603 | 2.039 | 2.652 | 2.133 |
| Quadratic + interactions | 0.923 | 0.930 | 0.894 | 2.492 | 3.172 | 2.812 | 1.914 | 2.775 | 2.285 |
| Cubic + interactions | 0.967 | 0.976 | 0.952 | 1.646 | 1.750 | 1.908 | 1.271 | 1.340 | 1.489 |

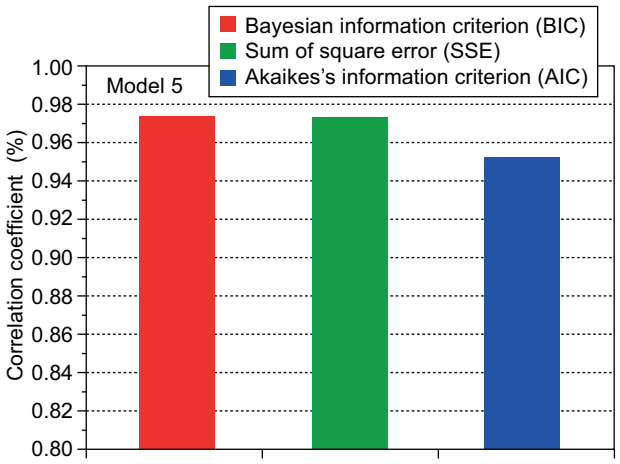


Figure 4. Comparing the CC of BIC, SSE and AIC.

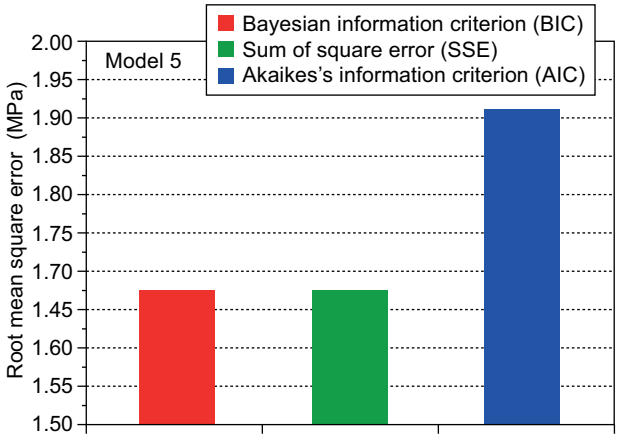


Figure 5. Comparing the RMSE of BIC, SSE and AIC.

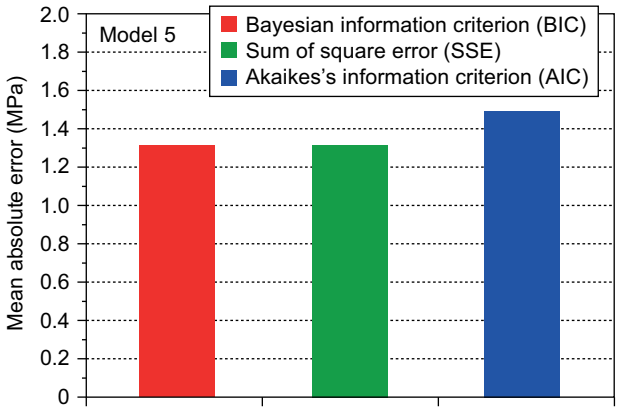


Figure 6. Comparing the MAE of BIC, SSE and AIC.

Figures 4, 5 and 6 depicted the CC, RMSE and MAE, respectively, for the developed cubic with interactions model (model V) using the BIC, SSE and AIC fitting criteria. Figure 4 compares the model using the CC as the accuracy criteria. The developed model using BIC and SSE showed similar performance and outperformed the model built with AIC by 2.8 %. When using the RMSE and MAE as the criteria to measure the accuracy of the model, the BIC and SSE showed similar performance as shown in Figures 5 and 6 and outperformed AIC by an improvement of 11.73 % and 13 % using the RMSE and MAE, respectively. Therefore, BIC was used as the fitting criterion throughout the remaining part of this paper.

## Predictive models for the compressive strength of the mixtures

The developed predictive models using the forward stepwise algorithm with the Bayesian information criterion (BIC) as the fitting criterion are presented in Equations 7 to 9. Equation 7 is for model I and II, Equation 8 is for model III and IV, while Equation 9 is for model V. The compressive strength of the mortar was expressed as a function of the binary binder variation ($x$), sodium hydroxide molarity ($M$), curing temperature ($T$), sodium silicate to sodium hydroxide ratio (NS/NH), alkaline to binder ratio [NS + NH)/BD], fine aggregate to binder ratio (FA/BD), water to binder ratio (W/BD) and the curing duration ($D$).

$$f'_c = -16.6 + 2.21M + 0.164T \tag{7}$$

$$\begin{aligned} f'_c = {} & 219.242 + 56.051x + 6.682M + 0.220T + \\ & + 23.727(\mathrm{NS/NH}) - 1114.001(\mathrm{AK/B}) + \\ & + 0.089D - 59.895x^2 - 0.235M^2 - \\ & - 15.394(\mathrm{NS/NH})^2 + 1107.851(\mathrm{AK/B})^2 \end{aligned} \tag{8}$$

$$\begin{aligned} f'_c = {} & 193.527 + 97.201x - 20.050M + 0.234T + \\ & + 3.554(\mathrm{NS/NH}) + 4.003(\mathrm{FA/B}) - \\ & - 784.843(\mathrm{AK/B}) + 1.581D - 0.285D(\mathrm{FA/B}) - \\ & - 159.349x^2 + 2.848M^2 + 19.199(\mathrm{NS/NH})^2 + \\ & + 778.693(\mathrm{AK/B})^2 - 0.079D^2 + 61.066x^3 - \\ & - 0.110M^3 - 14.733(\mathrm{NS/NH})^3 + 0.002D^3 \end{aligned} \tag{9}$$

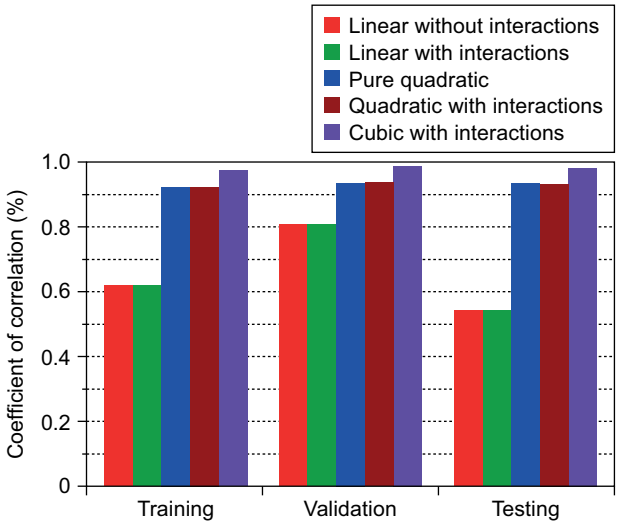


Figure 7. Comparison of the predictive strength of the stepwise regression models using the CC of the BIC.

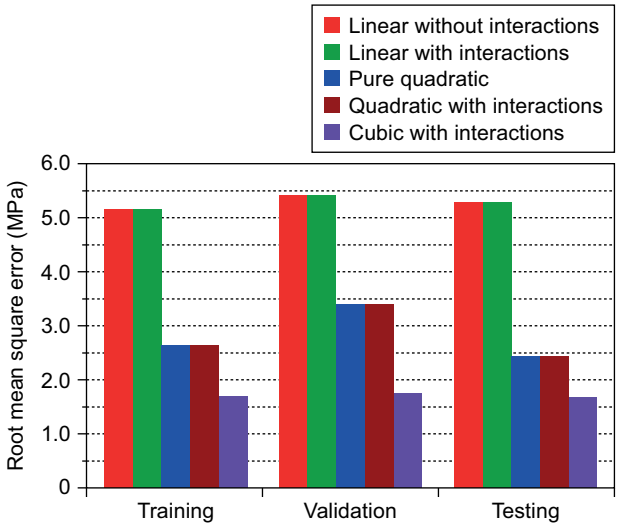


Figure 8. Comparison of the predictive strength of the stepwise regression models using. The root mean square error of the BIC.

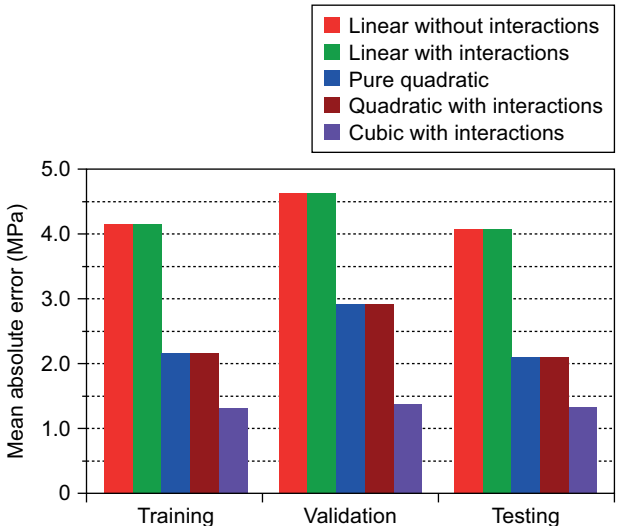


Figure 9. Comparison of the predictive strength of the stepwise regression models using. The mean absolute error of the BIC.

The efficiency of the proposed models during the training, validation and testing was evaluated using the correlation coefficient (CC), root means square error (RMSE) and means absolute error (MAE). Figures 7, 8 and 9 depicted the CC, RMSE and MAE, respectively, for all the developed predictive models. The linear without interactions model (model I) and the linear with interactions model (model II) only picked two input parameters (molarity and temperature) as the predictors (Equation 7), this causes the model to have low CC values of 61.4 %, 80.1 % and 53.6 % during the training, validation and testing, respectively, as shown in Figure 7.

However, when the order of the model changed to a second-order (model III and IV), the accuracy of the model improved by 48.86 %, 15.73 %, and 72.39 % for the training, validation and testing, respectively (Figure 7). The cubic with interactions model (model V) gave the best predictive model with accuracy of 96.6 %, 97 8 % and 97.2 % during the training, validation and testing of the developed model. RMSE values of 5.386, 5.263 and 5.263 were obtained during the training, validation and testing, respectively, for linear without interactions model (model I) and the linear with interactions model (model II) as shown in Figure 8. However, when the order of the model changed to a second-order (model III and IV), the RMSE values reduced by 48.74 %, 37.08 %, and 54.19 % for the training, validation and testing, respectively (Figure 8). The cubic with interactions model (model V) gave the best predictive model with the minimum RMSE of 1.682, 1.741 and 1.672 during the training, validation and testing of the developed model (Figure 8). Similar trends were observed using the MAE as shown in Figure 9. Model V showed excellent performance with the maximum CC and minimum RMSE and MAE when compared with the models (I-IV).

## Estimation of the compressive strength of the mixtures using Model 5

The correlation between the experimental and estimated compressive strength of the AALNMT of the developed cubic with the interaction model (model V) during the training section is depicted in Figure 10. The $R^2$-square value of 94.2 % was recorded as revealed in Figure 10. The $R^2$-square value of 94.3 % was obtained for the validation data as depicted in Figure 11 while the scatter plot for the testing stage showed an $R^2$-square value of 90.2 % as depicted in Figure 12. Generally, the estimated compressive strength for most of the data sets during the training, validation and testing were very close to the experimental values. Considering the high $R^2$-square value with the low RMSE and MAE of the testing, validation and testing data sets (Tab. 6), this points to the fact that the developed model is reliable, robust, accurate, and subsequently capable of estimating the compressive strength of the alkaline-activated mortar.

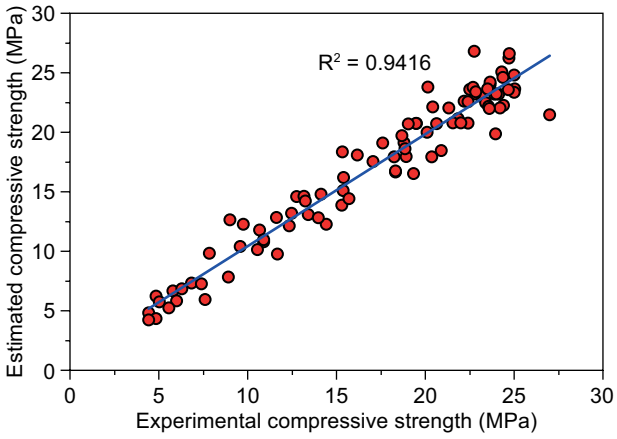


Figure 10. Scatter plots showing the performance of the training data set (model 5).

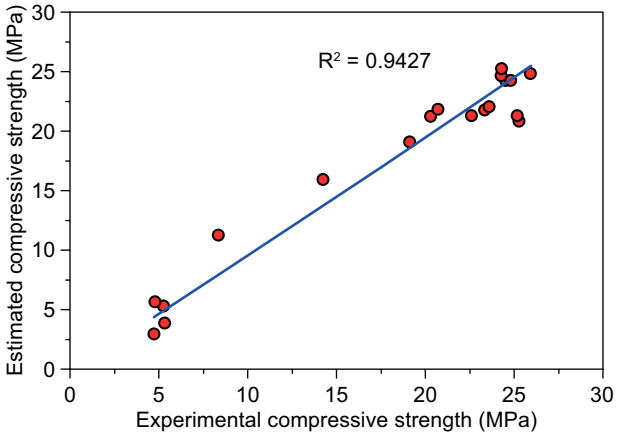


Figure 11. Scatter plots showing the performance of the validating data set (model 5).

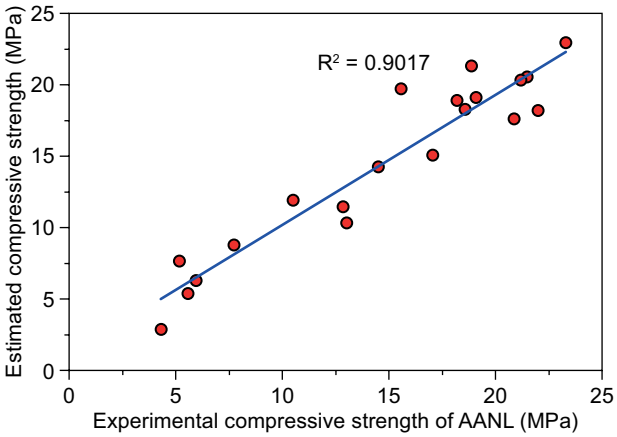


Figure 12. Scatter plots showing the performance of the testing data set (model 5).

## CONCLUSIONS

In this paper, we modelled the compressive strength of an alkali-activated natural pozzolan/limestone powder mortar (AALNM) using a stepwise regression algorithm. Five different models (model I = linear without interactions, model II = linear with interactions, model III = pure quadratic, model IV = quadratic with interactions and model V = cubic with interactions) were developed with seven descriptive features; the binary binder variation, sodium hydroxide molarity, curing temperature, sodium silicate to sodium hydroxide ratio, alkaline to binder ratio, fine aggregate to binder ratio, and the curing duration. The models were fitted using the Bayesian information criterion (BIC), Akaike's information criterion (AIC) and the sum of the square error (SSE) criteria. The results showed that the models developed using BIC and SSE have equal performance (CC = 0.972) and performed better than the predictive model with AIC (CC = 0.952). The generalisation strength of the developed models was investigated using the coefficient of correlations, root means square error and mean absolute error. Model V (cubic with interaction model) performed excellently, better than the other predictive models I-IV with an accuracy of 97.2 % measured on the basis of the correlation coefficient. Model V shows excellent results with a high coefficient of correlation, low root means square error and low mean absolute error. It also has a high potential for the quick and accurate estimation of the compressive strength of the mortar due to its excellent generalisation and predictive ability. Besides, the regression model developed would enhance the waste valorisation and judicious usage of the time deployed into the experimentation in the course of the synthesis of alkaline-activated binders.

## Acknowledgements

*The authors gratefully acknowledge the support from the Research Management Centre (RMC) Universiti Teknologi Malaysia (UTM), Ministry of Education of Malaysia Grant No: 5F066. The center for Engineering Research (CER) of the Research Institute, King Fahd University of Petroleum and Minerals, Dhahran, Saudi Arabia and the University of Hafr Al Batin, Hafr Al-Batin, Saudi Arabia.*

## REFERENCES

1. Duxson P., Provis J. L. (2008): Designing precursors for geopolymer cements. *Journal of the American Ceramic Society*, *91*(12), 3864-3869. doi: 10.1111/j.1551-2916.2008.02787.x
2. Damtoft J. S., Lukasik J., Herfort D., Sorrentino D., Gartner E. M. (2008): Sustainable development and climate change initiatives. *Cement and Concrete Research*, *38*(2), 115-127. doi: 10.1016/j.cemconres.2007.09.008
3. Andrew R.M. (2017). Global $CO_2$ emissions from cement production, pp. 1–52.
4. Van Damme, H. (2018): Concrete material science: Past, present, and future innovations. *Cement and Concrete Research*, *112*, 5-24. doi: 10.1016/j.cemconres.2018.05.002

5. Cwirzen A., Provis J. L., Penttala V., Habermehl-Cwirzen K. (2014): The effect of limestone on sodium hydroxide-activated metakaolin-based geopolymers. *Construction and Building Materials*, *66*, 53-62. doi: 10.1016/j.conbuildmat.2014.05.022
6. Provis J.L., van Deventer J.S.J. (2014). *Alkali avtivated materials*. Springer. doi: 10.1007/978-94-007-7672-2
7. Luukkonen T., Abdollahnejad Z., Yliniemi J., Kinnunen P., Illikainen M. (2018): One-part alkali-activated materials: A review. *Cement and Concrete Research*, *103*, 21-34. doi: 10.1016/j.cemconres.2017.10.001
8. Davidovits J. (2013). *Geopolymer Cement a review*. Geopolymer Institute, France. pp. 1–11
9. Najimi M., Ghafoori N., Sharbaf M. (2018): Alkali-activated natural pozzolan/slag mortars: A parametric study. *Construction and Building Materials*, *164*, 625-643. doi: 10.1016/j.conbuildmat.2017.12.222
10. Najimi M., Sobhani J., Ahmadi B., Shekarchi M. (2012): An experimental study on durability properties of concrete containing zeolite as a highly reactive natural pozzolan. *Construction and Building Materials*, *35*, 1023-1033. doi: 10.1016/j.conbuildmat.2012.04.038
11. Ibrahim M., Johari M. A. M., Maslehuddin M., Rahman M. K., Salami B. A., Mohamed H. D. (2019): Influence of composition and concentration of alkaline activator on the properties of natural-pozzolan based green concrete. *Construction and Building Materials*, *201*, 186-195. doi: 10.1016/j.conbuildmat.2018.12.117
12. Karim M. R., Zain M. F. M., Jamil M., Lai F. C. (2013): Fabrication of a non-cement binder using slag, palm oil fuel ash and rice husk ash with sodium hydroxide. *Construction and Building Materials*, *49*, 894-902. doi: 10.1016/j.conbuildmat.2013.08.077
13. Salami B. A., Johari M. A. M., Ahmad Z. A., Maslehuddin M. (2016): Impact of added water and superplasticizer on early compressive strength of selected mixtures of palm oil fuel ash-based engineered geopolymer composites. *Construction and Building Materials*, *109*, 198-206. doi: 10.1016/j.conbuildmat.2016.01.033
14. Kubba Z., Huseien G. F., Sam A. R. M., Shah K. W., Asaad M. A., Ismail, M., et al. (2018): Impact of curing temperatures and alkaline activators on compressive strength and porosity of ternary blended geopolymer mortars. *Case Studies in Construction Materials*, *9*, e00205. doi: 10.1016/j.cscm.2018.e00205
15. Salami B. A., Johari M. A. M., Ahmad Z. A., Maslehuddin M., Adewumi A. A. (2018): Impact of Al (OH) 3 addition to POFA on the compressive strength of POFA alkali-activated mortar. *Construction and Building Materials*, *190*, 65-82. doi: 10.1016/j.conbuildmat.2018.09.076
16. Yusuf M. O. (2015): Performance of slag blended alkaline activated palm oil fuel ash mortar in sulfate environments. *Construction and Building Materials*, *98*, 417-424. doi: 10.1016/j.conbuildmat.2015.07.012
17. Najamuddin S. K., Johari M. A. M., Maslehuddin M., Yusuf, M. O. (2019): Synthesis of low temperature cured alkaline activated silicomanganese fume mortar. *Construction and Building Materials*, *200*, 387-397. doi: 10.1016/j.conbuildmat.2018.12.056
18. Deb P. S., Nath P., Sarker P. K. (2014): The effects of ground granulated blast-furnace slag blending with fly ash and activator content on the workability and strength properties of geopolymer concrete cured at ambient temperature. *Materials & Design*, *62*, 32-39. doi: 10.1016/j.matdes.2014.05.001
19. Criado M., Aperador W., Sobrados I. (2016): Microstructural and mechanical properties of alkali activated Colombian raw materials. *Materials*, *9*(3), 158. doi: 10.3390/ma9030158
20. Lee N. K., Lee H. K. (2013): Setting and mechanical properties of alkali-activated fly ash/slag concrete manufactured at room temperature. *Construction and Building Materials*, *47*, 1201-1209. doi: 10.1016/j.conbuildmat. 2013.05.107
21. Sinthaworn S., Nimityongskul P. (2011): Effects of temperature and alkaline solution on electrical conductivity measurements of pozzolanic activity. *Cement and Concrete Composites*, *33*(5), 622-627. doi: 10.1016/j.cemconcomp.2011.02.012
22. Glasby T., Day J., Genrich R., Aldred J. (2015): EFC geopolymer concrete aircraft pavements at BrisbaneWest Wellcamp Airport, Concrete 2015. in: 27th Biennial National Conference of the Concrete Institute of Australia in Conjunction With the 69th RILEM Week, Melbourne, Australia. pp. 1051–1059. https://trid.trb.org/view/1394979
23. Van Deventer J. S., Provis J. L., Duxson P. (2012): Technical and commercial progress in the adoption of geopolymer cement. *Minerals Engineering*, *29*, 89-104. doi: 10.1016/j.mineng.2011.09.009
24. Mcintosh A., Lawther S.E.M., Kwasny J., Soutsos M.N., Cleland D., Nanukuttan S. (2015): Selection and characterisation of geological materials for use as geopolymer precursors. *Advances in Applied Ceramics*, *114*(7), 378-385. doi: 10.1179/1743676115y.0000000055
25. Patel R., Kinney F., Schumacher G. (2012). Green concrete using 100 % fly ash based hydraulic binder. in: *2012 International Concrete Sustainability Conference*. NRMCA, Seattle, USA. pp, 1–15. http://www.nrmcaevents.org/?nav=download&file=321
26. Cross D., Stephens J., Vollmer J. (2005).Structural Applications of 100 Percent Fly Ash Concrete. in: 2005 World Coal Ash, Montana State University, Bozeman, MT. pp. 1–19.
27. Jang J. G., Lee N. K., Lee H. K. (2014): Fresh and hardened properties of alkali-activated fly ash/slag pastes with superplasticizers. *Construction and Building Materials*, *50*, 169-176. doi:10.1016/j.conbuildmat.2013.09.048
28. Adewumi A. A., Owolabi T. O., Alade I. O., Olatunji S. O. (2016): Estimation of physical, mechanical and hydrological properties of permeable concrete using computational intelligence approach. *Applied Soft Computing*, *42*, 342-350. doi: 10.1016/j.asoc.2016.02.009
29. Ibrahim M., Johari M. A. M., Rahman M. K., Maslehuddin M. (2017): Effect of alkaline activators and binder content on the properties of natural pozzolan-based alkali activated concrete. *Construction and Building Materials*, *147*, 648-660. doi: 10.1016/j.conbuildmat.2017.04.163.
30. Değirmenci F. N. (2018): Utilization of natural and waste pozzolans as an alternative resource of geopolymer mortar. *International Journal of Civil Engineering*, *16*(2), 179-188. doi: 10.1007/s40999-016-0115-1
31. Adewumi A., Ismail M., Ariffin M. A. M., Yusuf M. O., Maslehuddin M., Mohamed H. D. (2019): Strength and microstructure of alkali-activated natural pozzolan and limestone powder mortar. *Инженерно-строительный журнал*, (8), 36-47. doi: 10.18720/MCE.92.3
32. Özcan A., Karakoç M. B. (2019): The resistance of blast furnace slag-and ferrochrome slag-based geopolymer con-

crete against acid attack. *International Journal of Civil Engineering*, *17*(10), 1571-1583. doi: 10.1007/s40999-019-00425-2

33. Behfarnia K., Rostami M. (2018): The effect of alkaline solution-to-slag ratio on permeability of alkali activated slag concrete. *International Journal of Civil Engineering*, *16*(8), 897-904. doi: 10.1007/s40999-017-0234-3
34. Atici U. (2011): Prediction of the strength of mineral admixture concrete using multivariable regression analysis and an artificial neural network. *Expert Systems with applications*, *38*(8), 9609-9618. doi: 10.1016/j.eswa.2011.01.156
35. Dahou Z., Castel A., Noushini A. (2016): Prediction of the steel-concrete bond strength from the compressive strength of Portland cement and geopolymer concretes. *Construction and Building Materials*, *119*, 329-342. doi: 10.1016/j.conbuildmat.2016.05.002
36. Öztaş A., Pala M., Özbay E., Kanca E., Caglar N., Bhatti M. A. (2006): Predicting the compressive strength and slump of high strength concrete using neural network. *Construction and Building Materials*, *20*(9), 769-775. doi: 10.1016/j.conbuildmat.2005.01.054
37. Alshihri M. M., Azmy A. M., El-Bisy M. S. (2009): Neural networks for predicting compressive strength of structural light weight concrete. *Construction and Building Materials*, *23*(6), 2214-2219. doi: 10.1016/j.conbuildmat.2008.12.003
38. Al-Khatib M. I., Al-Martini S. (2019): Predicting the rheology of self-consolidating concrete under hot weather. *Proceedings of the Institution of Civil Engineers-Construction Materials*, *172*(5), 235-245. doi: 10.1680/jcoma.16.00055
39. Asafa T. B., Adeniran A. A., Olatunji S. O. (2015): Functional networks models for rapid characterization of thin films: An application to ultrathin polycrystalline silicon germanium films. *Applied Soft Computing*, *28*, 11-18. doi: 10.1016/j.asoc.2014.11.058
40. Thomas R. J., Peethamparan S. (2017): Stepwise regression modeling for compressive strength of alkali-activated concrete. *Construction and Building Materials*, *141*, 315-324. doi: 10.1016/j.conbuildmat.2017.03.006.
41. ASTM Int. (2003).S *tandard Specification for Concrete Aggregates.* doi: 10.1520/C0033
42. ASTM Int. (2015). S*tandard Specification for Portland Cement*. pp. 1–6. doi: 10.1520/C0010